



Politecnico  
di Bari

Repository Istituzionale dei Prodotti della Ricerca del Politecnico di Bari

An Active Compensation System for the Temperature Dependence of SiPM Gain

This is a post print of the following article

*Original Citation:*

An Active Compensation System for the Temperature Dependence of SiPM Gain / Licciulli, Francesco; Marzocca, Cristoforo. - In: IEEE TRANSACTIONS ON NUCLEAR SCIENCE. - ISSN 0018-9499. - STAMPA. - 62:1(2015), pp. 228-235. [10.1109/TNS.2015.2388580]

*Availability:*

This version is available at <http://hdl.handle.net/11589/3226> since: 2021-03-08

*Published version*

DOI:10.1109/TNS.2015.2388580

*Terms of use:*

(Article begins on next page)

# An Active Compensation System for the Temperature Dependence of SiPM Gain

Francesco Licciulli and Cristoforo Marzocca

**Abstract**— Silicon Photo-Multiplier (SiPM) gain drifts due to temperature variations and this issue can be a source of relevant errors, for instance when the application requires high accuracy in the evaluation of the photopeak position, especially at low signal levels. In this paper we describe a compensation system that exploits a SiPM as temperature sensor and is able to keep the detector gain constant by means of fine adjustment of its bias voltage. The system is based on a feedback loop which measures the average amplitude of the dark pulses generated by the detector and compares it with a fixed reference, thus automatically correcting the device bias voltage and achieving constant amplitude of the dark pulses in presence of temperature variations. The same bias correction can be also applied to compensate the gain fluctuations of a SiPM not involved in the feedback loop, characterized by the same temperature dependence. The experimental results prove the effectiveness of the compensation system: for the SiPM used in the measurements, considering a temperature span of 10°C, the system is able to reduce the corresponding variation of the dark pulse amplitude from about 22% to only 0.78%.

**Index Terms**— SiPM, temperature compensation, gain stabilization.

## I. INTRODUCTION

**D**URING the last few years Silicon Photo-Multipliers (SiPM) have attracted increasing interest thanks to their useful properties, such as, just to name a few, high gain, good time resolution and low bias voltage, which contribute to expand the possible fields of application for these kind of detectors. Significant improvements of their performance have been achieved by continuous research advances, thanks to the introduction of new materials and technology processes, such as the use of metal instead of polysilicon for the quenching resistors [1]. Further progress is expected in the near future towards the mitigation of the main drawbacks which characterize SiPM detectors, such as dark pulse rate, optical crosstalk and afterpulsing.

One of the main downsides related to the SiPM behavior is the dependence of its gain on the temperature, due to the operating principle of the detector, based on the avalanche breakdown [2]. To keep the gain constant within the limits required by the application, the temperature of the SiPM must be accurately monitored and regulated by means of control systems, often complex and expensive. An interesting example of this kind of approach is given in [3], where an effective cooling system able to preserve the optical coupling between the scintillator and the detector is proposed. Another possible

option is the compensation of the gain deviations induced by the temperature variations by fine tuning the bias voltage of the detector. Different solutions have been proposed in the literature, based on this approach: in [4] and [5] the signal generated by a temperature sensor controls the SiPM bias voltage correction; in [6] and [7] thermistors have been inserted in the bias circuit of the SiPM to vary the detector bias voltage according to the temperature. In all these cases, to achieve good results in terms of stability of the detector gain, it is necessary to know with good accuracy both the temperature coefficient of the breakdown voltage of the SiPM and the conversion gain of the used temperature sensors, to balance out the opposite effects of the variations of bias voltage and temperature on the gain value.

Recently, we proposed a different approach for control and stabilization of the gain of a SiPM against temperature variations [8], based on the use of a SiPM of the same kind as a temperature sensor: the gain variation caused by the temperature fluctuation is monitored by measuring the peak value of the dark pulses generated by the SiPM and a negative feedback loop controls the fine adjustment of the detector bias voltage, to keep constant the amplitude of the dark pulses, thus achieving gain stabilization. A proof of principle for this approach has been also given in [8], using a complex experimental system not suitable for real applications, in which the algorithms for the evaluation of the bias voltage adjustments run on a host PC. In this paper, we develop a new experimental system which exploits the same operating principle but is suitable for application in a real environment, since it is based on simple analog circuit blocks. This makes possible, for instance, the integration of the system within a front-end ASIC intended for the read-out of SiPM detectors.

The paper organization is described in the following: in Section II the analytical relation between SiPM gain and temperature will be recalled and the conditions to be fulfilled to achieve a linear dependence between the amplitude of the dark pulses generated by a SiPM, coupled to the front-end electronics, and its breakdown voltage will be shown. In Section III the gain compensation system is presented, its main building blocks are described and the guidelines followed in the design of the system are reported. Last, in Section IV the experimental data that prove the effectiveness of the proposed gain compensation system are shown.

## II. DARK PULSE AMPLITUDE AND DETECTOR GAIN

The gain of a SiPM, defined as the charge delivered for a single photon event, normalized to the elementary charge, is given by the following relation:

F. Licciulli and C. Marzocca are with the Department of Electrical and Information Engineering, Politecnico di Bari, I70125 Bari, Italy (e-mail: cristoforo.marzocca@poliba.it).

$$G = \frac{C_{pixel}(V_{bias}-V_{BD})}{e}, \quad (1)$$

Where  $C_{pixel}$  and  $V_{BD}$  are respectively the total capacitance and the breakdown voltage of a single microcell of the sensor,  $V_{bias}$  is the bias voltage and  $e$  is the elementary charge. The gain depends on the temperature since the ionization energy needed to trigger the avalanche multiplication increases at higher temperature, due to higher probability of optical phonon scattering within the crystal lattice [9]. This phenomenon causes the increase of the breakdown voltage with the temperature [10]:

$$V_{BD}(T) = V_{BD0}[1 + \beta(T - T_0)] \quad (2)$$

where  $V_{BD0}$  is the breakdown voltage measured at a reference temperature  $T_0$  and  $\beta$  is a coefficient that can assume values in the order of  $10^{-3}/^{\circ}C$ . In order to keep constant the gain with the temperature the overvoltage  $\Delta V = V_{bias} - V_{BD}$ , must be kept constant, by changing the bias voltage according to the  $V_{BD}$  variation.

It is possible to exploit the dark current thermally produced by the SiPM to monitor its gain variation. Direct measurements of the average charge associated to the dark pulses are not statistically reliable because their accuracy is affected by several errors, such as afterpulsing and excess noise. Moreover, the dark rate increases with both temperature and overvoltage, which makes it difficult to measure the charge contained in a single pulse, due to the increased pile up probability. These considerations are confirmed by Fig. 1(a), which reports the mean value of the dark pulse charge as a function of bias voltage and temperature for a  $3 \times 3 \text{ mm}^2$  SiPM from Hamamatsu, read-out by means of an amplifier with input resistance  $R_s = 25\Omega$  and bandwidth  $BW = 20\text{MHz}$ . On the other hand, Fig. 1(b) shows that measurements of the peak value of the dark pulses are much more reliable to evaluate the detector gain variations as a function of temperature and bias voltage, especially when the temperature increases. Note that Fig 1(a) and (b) have been obtained considering the same set of 1000 dark pulses for each reported experimental point.

It is possible to demonstrate that, under particular conditions, the average amplitude of the dark pulses is linearly dependent on the overvoltage and the temperature, thus can be used to monitor the variations of the detector gain.

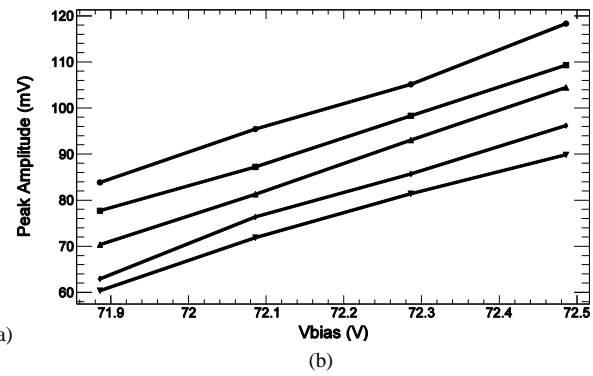
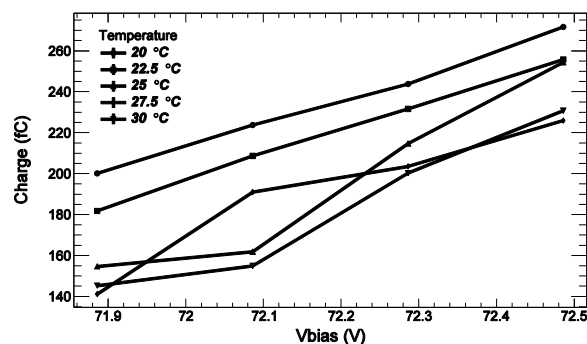


Fig. 1. Comparison between mean charge (a) and mean peak voltage (b) for dark pulses at different bias voltages and temperature for a 3600 microcells SiPM from Hamamatsu (S10931-050P).

A well-known low frequency model of the SiPM coupled to the front-end electronics [11], shown in Fig. 2, can be exploited to carry out this analysis.

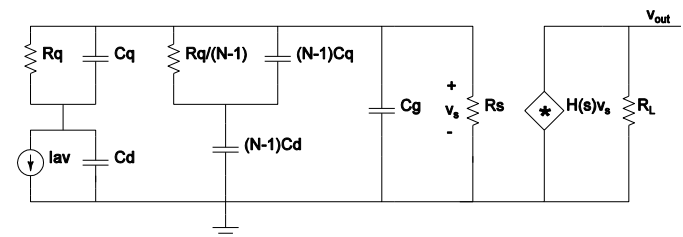


Fig. 2. Electrical model of the SiPM coupled to the front-end electronics.

In Fig. 2, the front-end electronics is modelled by the generic source  $H(s)v_s$ , which can be a current or a voltage according to the chosen preamplifier structure, controlled by the voltage across its input resistance  $R_s$ .  $C_d$  is the photodiode capacitance,  $R_q$  is the quenching resistor with its parasitic capacitance  $C_q$ ,  $C_g$  is the parasitic capacitance associated to the metal grid used to interconnect the microcells,  $N$  is the total number of microcells that compose the SiPM.  $I_{av}$  is a current source which models the very fast current pulse generated by the single microcell undergoing avalanche breakdown and can be approximated as a Dirac's delta with amplitude  $Q_0 = eG$ .

In Appendix I the entire derivation of an approximate expression for the output pulse  $v_{out}(t)$  and the calculation of its peak value  $v_{max}$  are fully developed. The final expressions of  $v_{out}(t)$  and  $v_{max}$  are reported in (3) and (4) respectively.

$$v_{out}(t) = f_{s1}e^{-p_1t} + f_{s2}e^{-p_2t} + f_{sA}e^{-p_At} \quad (3)$$

$$v_{max} = \left[ K_1(B)^{\frac{p_1}{p_2-p_A}} + K_2(B)^{\frac{p_2}{p_2-p_A}} + K_A(B)^{\frac{p_1}{p_2-p_A}} \right] \Delta V = K\Delta V \quad (4)$$

Here  $p_1$  and  $p_2$  are the two poles of the circuit in Fig. 2: their approximated expressions, valid under the hypothesis that the input resistance of the preamplifier  $R_s$  is small enough (see

Appendix I), are the following:

$$p_1 = \frac{1}{R_s(C_{eq}+C_g)}, \quad p_2 = \frac{1}{R_q(C_d+C_q)}, \quad (5)$$

$$\text{where } C_{eq} = N \frac{C_d C_q}{C_d + C_q}.$$

Moreover,  $p_A$  represents the pole of the transfer function of the preamplifier, considered as a first order system:

$$\frac{V_{out}}{V_s}(s) = A_0 \frac{p_A}{s + p_A}$$

Last,  $K_i$ ,  $f_{si}$  ( $i=1,2,A$ ) and  $B$  are constants which depend only on parameters of the SiPM and the front-end electronics, thus the linearity of the relationship between the amplitude of the dark pulses and the overvoltage  $\Delta V$  is confirmed by (4).

Note that, as explained in Appendix I, the approximate expression (4) holds true only if the values of the bandwidth and the input resistance of the front-end electronics are carefully selected. If  $BW$  and  $R_s$  are increased, the results of the approximated analysis can be affected by a large error and the amplitude of the dark pulses does not exhibit a linear behavior as a function of  $\Delta V$ , thus the peak value cannot be used as a measurement of the SiPM gain. In order to study this issue, the results provided by (4) and by simulations carried out on the circuit in Fig. 2 have been compared, varying the bandwidth and the input resistance of the preamplifier. Fig. 3 reports the error obtained between the amplitude of the dark pulses achieved from SPICE simulations and from (4), using the parameters of the Hamamatsu S10931-050P. For example, considering  $R_s = 25\Omega$ , the percent error spans from  $30 \cdot 10^{-6}\%$  to 40% when the bandwidth is varied between 10MHz and 115MHz. This error analysis can be useful to choose a suitable pair  $(R_s, BW)$  for the front-end electronics to be used if we want to evaluate the gain of the detector via measurements of dark pulse amplitude, which is the basic principle of the proposed gain compensation method.

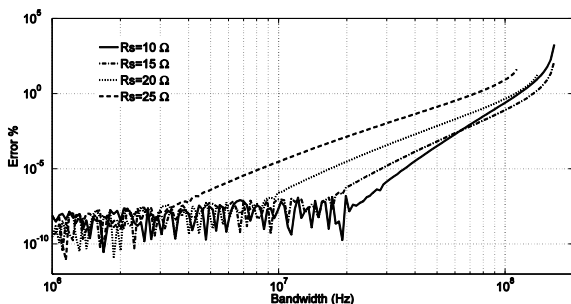


Fig. 3. Error between the results provided by (4) and by SPICE simulations of the circuit in Fig. 2 as a function of the bandwidth and the input resistance of the front-end electronics.

### III. TEMPERATURE COMPENSATION SYSTEM

The schematic diagram of the proposed compensation system is shown in Fig. 4. The SiPM in Fig. 4 is used only as a temperature sensor and must generate only dark pulses, thus

photons must be prevented from reaching the detector.

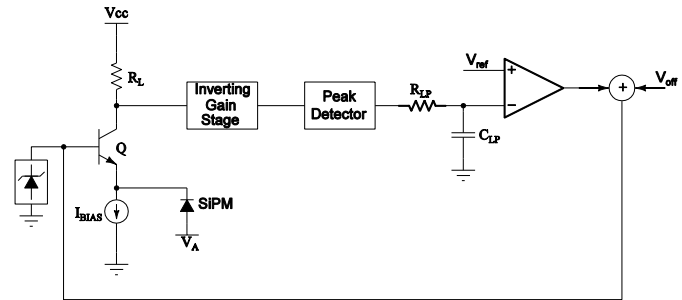


Fig. 4. Temperature compensation system architecture: in the proposed scheme, a current-mode front-end circuit has been considered.

The front-end is a transimpedance preamplifier, composed by a current buffer realized by means of the NPN BJT and the resistor  $R_L$ , which converts the SiPM dark pulses into a voltage. This kind of front-end has been chosen only as an example and the proposed compensation method can be applied also in case a different kind of preamplifier is used to read out the SiPM, provided that an input for the fine tuning of the detector bias voltage is available. In any case the bandwidth of the preamplifier used in the temperature compensation circuit must be suitably limited, as discussed above. The front-end is followed by a gain stage, an operational amplifier THS4051 in inverting configuration, which amplifies the dark pulses. The current buffer configuration allows a very easy fine adjustment of the SiPM bias voltage, since a variation of the base voltage of the BJT is followed by the emitter, which is DC coupled to the detector.

The peak detector measures the peak value of the dark pulses and the following low pass filter  $R_{LP}-C_{LP}$  extracts the average value of the peak amplitude. The resulting signal is compared with a fixed reference  $V_{ref}$ , representing the set-point of the feedback system, by means of a differential amplifier which generates the feedback signal. An offset  $V_{off}$  is added to the feedback signal and the feedback loop is closed to the base of the input transistor. A temperature change causes the variation of the average value of the peak amplitude and, as a consequence, the feedback signal changes the base voltage of the input transistor, followed by the emitter voltage. If the loop gain of the feedback system is large enough, the resulting variation of the SiPM bias voltage is able to keep constant the mean amplitude of the dark pulses generated by the detector, thus accomplishing the sensor gain control. Furthermore, by changing the value of  $V_{ref}$ , the system is able also to set the desired value of the SiPM overvoltage and, as a consequence, of its gain.

The input front-end must be designed in order to fulfill the conditions required to obtain a linear dependence between the SiPM overvoltage and the peak value, according to (4). The bias current of the input transistor sets the desired value for the input resistance of the front-end  $R_s=1/g_m$ , where  $g_m$  is the transconductance of the BJT. The bandwidth of the gain stage must be conveniently reduced, as discussed in the previous

section, thus noise is not of particular concern, also due to the large gain of the detector. Last, the load resistor  $R_L$  and the gain of the following amplifier are selected to achieve a suitable peak value.

The peak detector must be able to process low amplitude pulses and its discharge time constant  $\tau_{PD}$  must be selected according to the mean rate of the single dark pulses. The rate of double or higher order dark pulses is much smaller, thus they do not affect significantly the signal at the output of the low pass filter, if  $\tau_{PD}$  is not too large. Moreover, since the single dark pulse rate is always much faster than the temperature variations, the peak detector output, averaged by the low-pass filter, is always able to provide an up-to-date information of the temperature behavior.

The circuit structure of the peak detector is represented in Fig. 5. As soon as the input voltage starts decreasing, the comparator fires and the switch is opened, so that the output voltage evolves according to the slow time constant  $\tau_{PD}=R_{PD}C_{PD}$ , starting from the peak value. In our implementation of the circuit, an OPA1611 has been used for the buffer stage, the comparator is a TLS3501 and the controlled switch is a TS5A1066.

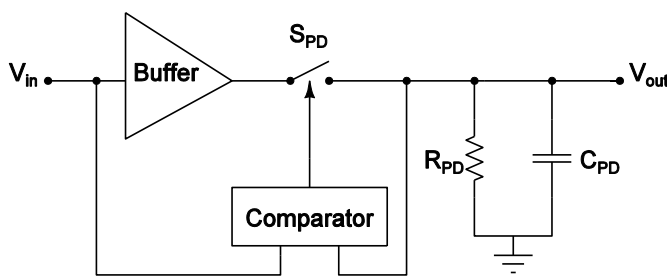


Fig. 5. Schematic structure of the peak detector.

To choose a proper value for the discharging time constant of the peak detector  $\tau_{PD}$ , extensive Monte Carlo simulations of the dark pulse generation process have been carried out, corresponding to different  $\tau_{PD}$  values and dark pulse rates. The parameter  $K_{PD}$ , defined as the ratio between the integral of the peak detector output and the product of the simulation time and the single dark pulse peak amplitude has been chosen as a parameter useful to measure the effectiveness of the information provided by the average value of the peak detector output. For a given dark rate, the optimal value of  $K_{PD}$  is one: if  $\tau_{PD}$  is too small, the peak detector will not be able to store the peak value between two consecutive pulses and  $K_{PD}$  will be much smaller than one; for too large values of  $\tau_{PD}$ , higher order dark pulses will cause  $K_{PD}$  values much larger than one. Since  $K_{PD}$  is a function of the dark rate, the optimal value of  $\tau_{PD}$  depends on the specific SiPM. On the other hand, dark rate is a function of the temperature, which means that also the parameter  $K_{PD}$  is affected by temperature variations. In case the temperature span is restricted to an interval of about  $10^\circ\text{C}$ , as happens in several applications, the variation of  $K_{PD}$  is negligible, thus the peak detector output represents a reliable signature of the average single dark pulse amplitude.

Fig. 6 shows the typical behavior of  $K_{PD}$  as a function of  $\tau_{PD}$  corresponding to different values of dark rate. Only one Monte Carlo trial, i.e. one possible realization of the dark pulse generation process, has been reported in Fig. 6 for each considered dark rate value.

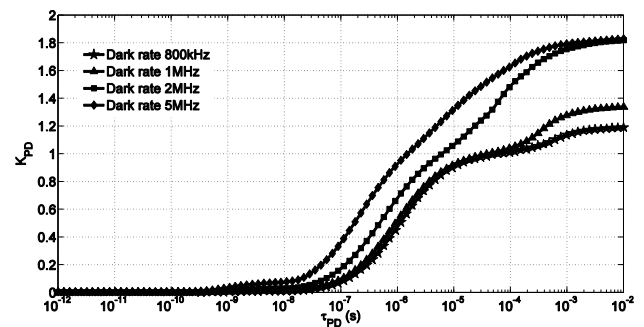


Fig. 6. Simulations of the parameter  $K_{PD}$  as a function of peak detector discharge time constant  $\tau_{PD}$  for different dark pulse rates.

The low pass filter  $R_{LP}-C_{LP}$  has a very slow time constant that allows the measure of the average value of the peak over a long time interval and, at the same time, guarantees the stability of the feedback loop, since it corresponds to the dominant pole of the loop. In fact, a single pole frequency behavior is required to get a loop gain with a sufficiently large phase margin.

An OPAMP based adder has been used to sum the constant offset  $V_{off}$  to the feedback signal. The offset is needed to make sure that all the components in the feedback loop work in a convenient operating point, so that the differential amplifier operates in its linear range. A limiting circuit based on a zener diode has been used to limit the voltage at the base of the BJT, since during the initial transient, when the difference between the low pass filter output and the set-point value is large, the differential stage output could cause the saturation of the input stage and the feedback loop would not be able to recover the correct operating point.

Note that two different feedback loops are established in the system of Fig. 4. The first one is closed through the SiPM, thanks to the dependence of the peak value of the dark pulses on the bias voltage of the detector. The second feedback loop does not involve the SiPM and is closed via the input BJT, configured as an inverting stage with negligible gain, due to the presence of the constant current source  $I_{BIAS}$ , realized by means of a cascode current mirror. As a consequence, the associated loop gain is also very low and this “parasitic” feedback loop does not give significant contributions to the behavior of the compensation system.

In case the SiPM is biased under the breakdown voltage, no dark pulses are generated and the peak detector output is zero. The voltage at the output of the differential amplifier is positive and large and the limiting zener diode avoids saturation of the front-end stage. When the detector is biased over the breakdown voltage and starts to operate in Geiger mode, the main feedback loop controls the average amplitude of the dark pulses to the set-point value  $V_{ref}$ .



If the conditions which guarantee the validity of (4) are fulfilled, the relationship between the base voltage of the input BJT and the peak detector output can be considered linear. The steady state error of the feedback loop is thus defined as:

$$e_{pk} = V_{ref} - v_{max} \quad (6)$$

and, by applying (4), its complete expression is the following:

$$e_{pk} = \frac{V_{ref}}{1 + KA_D} - \frac{K}{1 + KA_D} (V_{off} - V_{BE} - V_A - V_{BD0}) + \frac{K}{1 + KA_D} \beta \Delta T \quad (7)$$

where  $K$  is the constant factor which appears in (4),  $A_D$  is the gain of the differential stage,  $V_{BE}$  is the base-emitter voltage of the input transistor and  $\Delta T = T - T_0$ . The first two terms of (7) represent a constant contribution to the error, whereas the third one is depending on the temperature. The error  $e_{pk}$  can be reduced by choosing a suitable value for  $A_D$ , which can be different if we want to make negligible only the temperature dependent term in (7) or if we want to achieve also an accurate value of  $v_{max} \cong V_{ref}$ .

In order to study the stability of the main feedback loop, the gain-bandwidth product  $GBW$  of the loop gain can be evaluated:

$$GBW = KA_D f_{LP} \quad (8)$$

where  $f_{LP}$  is the low pass filter cut-off frequency, which is the dominant pole in the loop. The phase margin of the system depends on the position of the poles introduced by the other blocks, i.e. the transimpedance input stage, the differential amplifier and the analog adder. In our case the instrumentation amplifier AD8421 that has been used as error amplifier is the source of the second pole of the loop and the cut-off frequency of the low pass filter has been set to obtain a  $90^\circ$  phase margin.

The  $GBW$  of the loop gain represents also the cut-off frequency of the closed loop transfer function, which limits the fastest temperature variation that can be compensated. Our system has  $GBW = 1.7\text{kHz}$  with  $90^\circ$  of phase margin, achieved with a low pass filter cut-off frequency of  $23\text{Hz}$ .

#### IV. EXPERIMENTAL RESULTS

The experimental setup developed to test the proposed compensation system has been assembled in a dark box and exploits a Peltier cell to control the temperature of two SiPMs: one of the two detectors is used as temperature sensor and is enclosed in the feedback loop discussed in the previous section, whereas the other, which is out of the feedback loop but is biased by means of the same feedback control signal generated by the loop, is used to prove the effectiveness of the proposed compensation system. Both detectors are read-out by means of the same kind of transimpedance amplifier, based on

the common base stage considered in the previous section. The dark pulses generated by the second detector are digitized and the peak pulse spectra have been measured for different temperatures with the compensation system both activated and disabled.

The employed detectors are  $3 \times 3\text{mm}^2$  S10931-050P Hamamatsu devices with 3600 microcells  $50\mu\text{m} \times 50\mu\text{m}$ . For both SiPMs the temperature dependence of the breakdown voltage  $V_{BD}$  has been extracted by measurements carried out with a semiconductor parameter analyzer and the results are reported in Fig. 7. The statistical uncertainty of the measured points in Fig. 7 is negligible and the measurements exhibit very good repeatability. The linear fitting of the measured data shown in Fig. 7 yields a breakdown voltage temperature coefficient  $\beta$  for the two devices equal to  $44\text{mV}/^\circ\text{C}$  and  $40\text{mV}/^\circ\text{C}$  respectively, which are rather different from the one reported in the data sheet of the devices ( $56\text{mV}/^\circ\text{C}$ ), probably due to different methods used to extract the value of  $V_{BD}$ . In any case the proposed compensation approach is not based on the absolute value of  $\beta$ , thus the method used to estimate it does not affect its effectiveness.

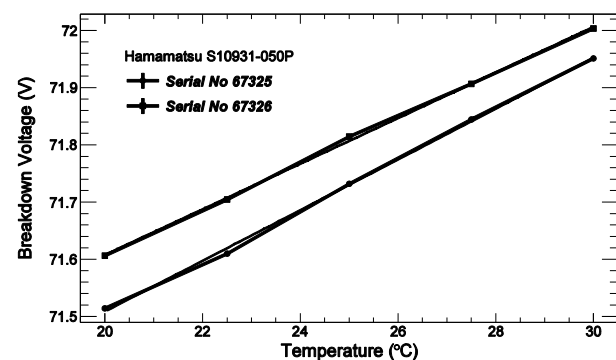


Fig. 7. Temperature dependence of the breakdown voltage for the two SiPMs employed in the experimental setup, with the corresponding linear fits.

Considering Fig. 7, it is apparent that the two SiPMs are not perfectly matched, in terms of both  $V_{BD0}$  and  $\beta$ . The mismatch between the breakdown voltages  $V_{BD0}$  does not affect at all the behavior of the temperature compensation system, whereas the difference between the temperature coefficients  $\beta$  of the two devices results in a small residual dependence of the gain of the second SiPM on the temperature variations. Nevertheless, this phenomenon is common to all the possible temperature compensation schemes in which variations of the common bias voltage of the detectors are used to compensate the breakdown voltage variations induced by temperature drifts.

In our experiments, first the temperature of the detectors has been set at a constant value by means of the Peltier; next 1000 dark pulses generated by the out-of-the-loop detector have been digitized and analyzed to monitor its gain. The temperature has been controlled in the interval between  $20^\circ\text{C}$  and  $30^\circ\text{C}$  with a step of  $2.5^\circ\text{C}$ . This measurement procedure has been adopted since our temperature controller was not able to reproduce time-temperature profiles. Anyway, the procedure provides significant results in terms of effectiveness

of the temperature compensation technique. In fact, in all the actual applications the temperature variations are very slow with respect to the time constant of the low pass filter employed in the system and, at the same time, the dark rate of the detectors is always large enough to make sure that the averaging operation carried out by the filter is performed on a significant number of dark pulse samples, as already pointed out in the previous section. For the SiPMs used in our system the order of magnitude of the dark rate is 1MHz.

Fig. 8 refers to data obtained when the compensation system is disabled and the bias voltage of the out-of-the-loop SiPM is kept constant with the temperature. For this detector, the spectra of the dark pulse amplitude, normalized to the highest mean peak value (corresponding to 20°C), are reported along with their Gaussian fittings. As expected, the average peak value shifts towards lower values as temperature increases from 20°C to 30°C.

In all the measurements carried out when the compensation system is active, the two SiPMs have been biased with an initial voltage of 73V, established by the zener diode, and the feedback loop controls the bias voltage of the in-the-loop device, so that the average amplitude of its dark pulses reaches the set-point reference and is kept constant when the temperature changes. Fig. 9 shows the spectra of the dark pulse amplitudes generated by the out-of-the-loop SiPM at different temperatures when this device is biased with the same voltage of the in-the-loop detector, so the compensation system is active. The shift in the mean peak value of the dark pulses as a function of the temperature is much smaller than in Fig. 8, which means that the gain of the detector is much more stable. The distributions shown in Fig. 9 exhibit more pronounced tails in the region corresponding to high values of the amplitude, compared to the ones reported in Fig. 8. This is due to the set point chosen in the closed loop measurements, which produces a SiPM overvoltage constant with the temperature, but larger than the one, variable with the temperature, corresponding to the open loop measurements in Fig. 8.

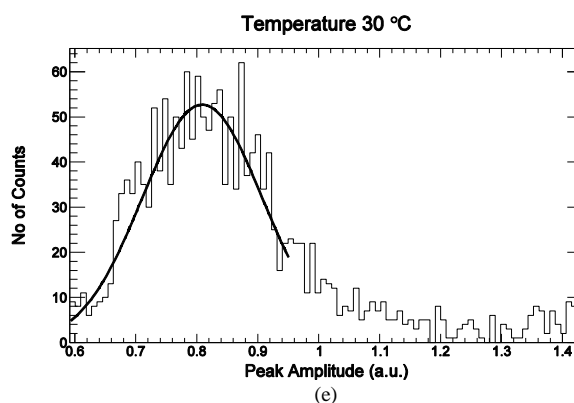
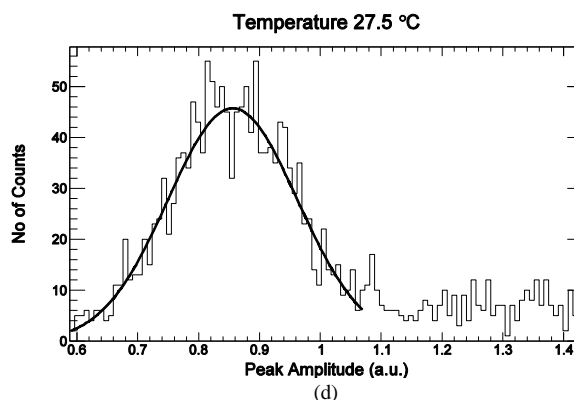
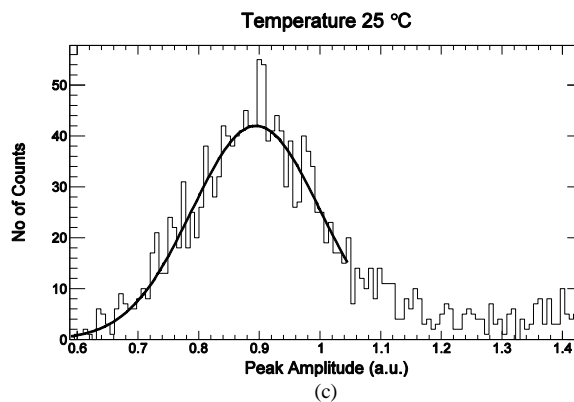
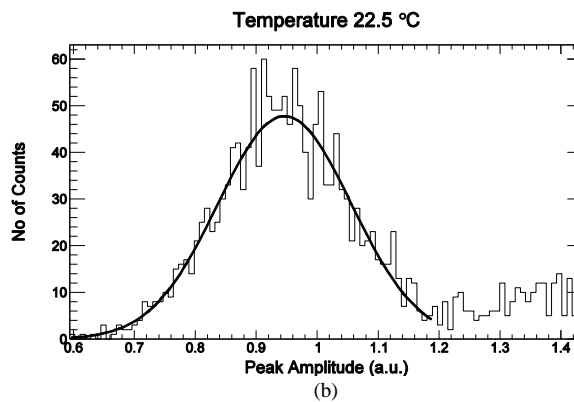
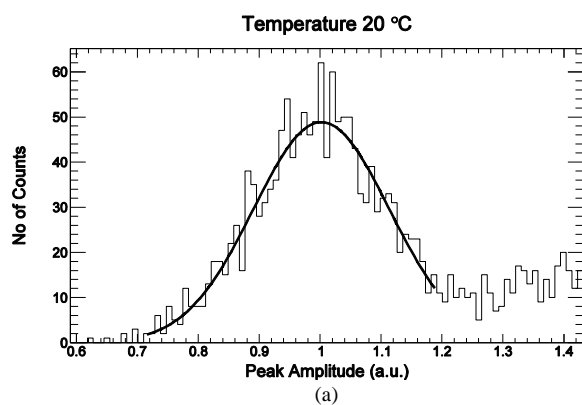


Fig. 8. Peak spectra measured when the compensation system is disabled, for different temperatures: 25°C (a), 22.5 °C (b), 25 °C (c), 27.5 °C (d), 30 °C (e).

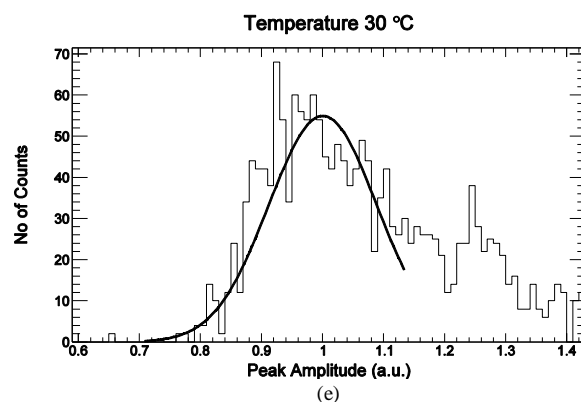
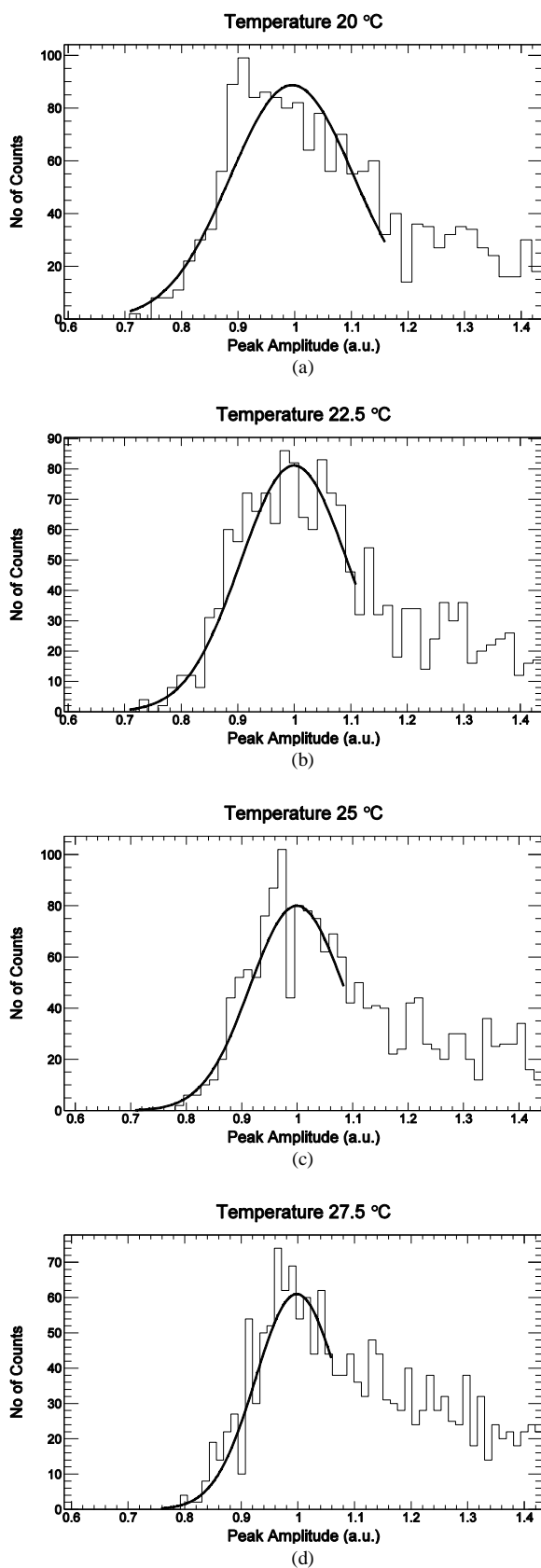


Fig. 9. Peak spectra measured when the compensation system is active, for different temperatures: 25 °C (a), 22.5 °C (b), 25 °C (c), 27.5 °C (d), 30 °C (e).

Fig. 10 shows a comparison between the average peak values extracted from Figs. 8 and 9 as a function of the temperature. When the temperature compensation system is active the maximum relative variation of the average amplitude of the dark pulses is about 0.78%, compared to a value of about 22% in case the system is disabled. The same variations, of course, are experienced by the gain of the out-of-the-loop SiPM.

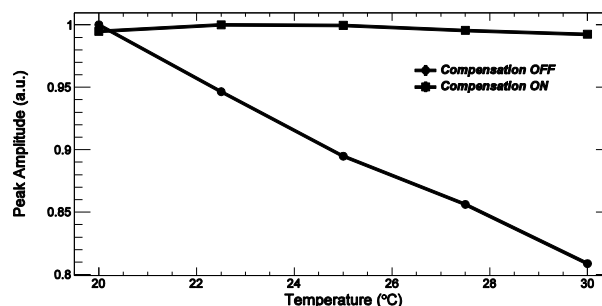


Fig. 10. Comparison between peak values measured in case of compensation system active and disabled.

Last, it is also interesting to observe that it is not necessary to use the same bias level  $V_A$  for the two detectors, which must share only the same bias variation. In other words, the compensation system works correctly also if the gain of the SiPM used as temperature sensor is set at a different value with respect to the gain chosen for the out-of-the-loop detector. Moreover, the two SiPMs can also operate at different absolute temperatures and the only requirement for the effectiveness of the compensation system is that they must experience the same temperature variations, which is a less difficult condition to be fulfilled in a practical situation. This can represent a relevant advantage in terms of flexibility in a real application in which a matrix of out-of-the-loop SiPMs experiences the same bias voltage variations of the “blind” SiPM used as a temperature sensor device, but is not forced to share the same absolute value of bias voltage or temperature.



## V. CONCLUSION

A compensation system to make stable the gain of SiPM detectors against temperature variations has been proposed and its hardware implementation has been described. The conditions to be fulfilled in order to guarantee its effectiveness have been discussed and, since the system is based on a negative feedback loop, the issues related to its stability have also been addressed. Experimental results, obtained considering a system composed by two detectors, show that the compensation system is able to keep the gain variation lower than 0.78% over a range of 10°C. The proposed architecture can be used in a detection system to stabilize the gain of an array of SiPMs against temperature drifts: in this case one of the pixels of the matrix can be conveniently covered to prevent the absorption of photons and used as temperature sensor in the feedback loop, whereas the bias variations generated by the loop can be applied to the other detectors of the matrix. Large detection systems can be partitioned in separate sections working at different local temperatures, each served by its own temperature compensation system.

## APPENDIX I

Considering Fig. 2, the voltage across  $R_s$ , in the Laplace domain, is equal to:

$$V_S(s) = K_{mol} \frac{s+z}{(s+p_1)(s+p_2)},$$

where

$$z = \frac{1}{R_q C_q},$$

$$p_1 = \frac{1}{R_s(C_{eq} + C_g)}, \quad p_2 = \frac{1}{R_q(C_d + C_q)}$$

$$\text{and } K_{mol} = R_s C_q p_1 \Delta V = \frac{C_q}{C_{eq} + C_g} \Delta V.$$

The expressions for the poles  $p_1$  and  $p_2$  have been obtained under the following hypothesis:

$$R_s(C_g + NC_d) \ll R_q(C_d + C_q),$$

which holds true if the value of  $R_s$  is small enough.

Assuming a single pole transfer function for the front-end, the output voltage of the preamplifier is:

$$V_{out}(s) = A_0 \frac{p_A}{s+p_A} V_S(s) \quad (A1)$$

$A_0$  can be a voltage gain, in case the controlled source  $H(s)v_S$  in Fig. 2 is a voltage, or  $A_0 = G_m R_L$  in case  $H(s)v_S$  is a current.

The inverse Laplace transform of (A1) is:

$$v_{out}(t) = f_{s1} e^{-p_1 t} + f_{s2} e^{-p_2 t} + f_{sA} e^{-p_A t} \quad (A2)$$

where:

$$f_{s1} = K_{mol} A_0 p_A \frac{z - p_1}{(p_2 - p_1)(p_A - p_1)}$$

$$f_{s2} = K_{mol} A_0 p_A \frac{z - p_2}{(p_1 - p_2)(p_A - p_2)}$$

$$f_{sA} = K_{mol} A_0 p_A \frac{z - p_A}{(p_1 - p_A)(p_2 - p_A)}$$

The time response  $v_{out}(t)$  is composed by three exponentials. In order to evaluate the peaking time and the peak value, the exponential related to the pole  $p_1$  is assumed to be much faster than the other poles, so its contribution to the peak value can be considered negligible. In the design phase, the values of  $R_s$  and  $p_A$  can be chosen in order to guarantee the validity of this assumption.

The approximated output voltage, neglecting the fast exponential, is:

$$v_{out}(t) \cong f_{s2} e^{-p_2 t} + f_{sA} e^{-p_A t} \quad (A3)$$

from which the peaking time expression is:

$$t_{max} = \frac{1}{p_2 - p_A} \ln \left( -\frac{p_2 f_{s2}}{p_A f_{sA}} \right) \quad (A4)$$

Replacing (A4) in (A2) the final approximated expression for the peak value of  $v_{out}(t)$  has been reported in (4) and is the following one:

$$v_{max} = \left[ K_1(B) \frac{p_1}{p_2 - p_A} + K_2(B) \frac{p_2}{p_2 - p_A} + K_A(B) \frac{p_1}{p_2 - p_A} \right] \Delta V = K \Delta V$$

where

$$B = -\frac{p_A f_{sA}}{p_2 f_{s2}}$$

$$K_1 = A_0 R_s C_q p_1 p_A \frac{z - p_1}{(p_2 - p_1)(p_A - p_1)}$$

$$K_2 = A_0 R_s C_q p_1 p_A \frac{z - p_2}{(p_1 - p_2)(p_A - p_2)}$$

$$K_A = A_0 R_s C_q p_1 p_A \frac{z - p_A}{(p_1 - p_A)(p_2 - p_A)}$$

## REFERENCES

- [1] *Technical Information - MPPC, MPPC modules*, Hamamatsu Photonics K.K., Japan, available: [https://www.hamamatsu.com/resources/pdf/ssd/mppc\\_techinfo\\_e.pdf](https://www.hamamatsu.com/resources/pdf/ssd/mppc_techinfo_e.pdf) technical information.
- [2] M. Ramilli, "Characterization of SiPM: temperature dependencies", *2008 IEEE Nucl. Sci. Symp. and Med. Imag. Conf. Record*, Dresden, pp. 2467-2470, 2008.
- [3] A.V. Stolin, S. Majewski, R.R. Raylman, "Novel Method of Temperature Stabilization for SiPM-Based Detectors", *IEEE Trans. Nucl. Sci.*, vol. 60, no. 5, pp. 3181-3187, 2013.

- [4] P. S.Marrocchesi, M. G. Bagliesi et al., "Active Control of the Gain of a 3mm x 3mm Silicon PhotoMultiplier", *Nucl. Instr. Meth. in Phys. Res. Sec. A*, vol. A602, pp. 391-395, 2009.
- [5] R. Bencardino and J. E. Eberhardt, "Development of a Fast-Neutron Detector with Silicon Photomultiplier Readout", *IEEE Trans. Nucl. Sci.*, vol. 56, no. 3, pp. 1129-1134, 2009.
- [6] H. Miyamoto, M. Teshima, "SiPM development for the imaging Cherenkov and fluorescence telescopes", *Nucl. Instr. Meth. in Phys. Res. A*, vol. A623, pp. 198-200, 2010.
- [7] Zhengwei Li, Yupeng Xu, Congzhan Liu, et. al., "A gain control and stabilization technique for Silicon Photomultipliers in low-light-level applications around room temperature", *Nucl. Instr. Meth. in Phys. Res. A*, vol. A695, pp. 222-225, 2012.
- [8] F. Licciulli, I. Indiveri, C. Marzocca, "A novel technique for the stabilization of SiPM gain against temperature variations", *IEEE Trans. Nucl. Sci.*, vol. 60, no. 2, pp. 606-611, 2013.
- [9] C.Y. Chang, S.S. Chiu, L.P.Hsu, "Temperature dependence of breakdown voltage in silicon abrupt p-n junctions", *IEEE Trans. El. Dev.*, vol. 18, no. 6, pp. 391-393, 1971.
- [10] K. G. McKay, "Avalanche breakdown in silicon," *Phys. Rev.*, vol. 94, pp. 877-884, 1954..
- [11] F. Corsi, A. Dragone, C. Marzocca, A. Del Guerra, P. Delizia, N. Dinu, C. Piemonte, M. Boscardin, G.F. Dalla Betta, "Modelling a silicon photomultiplier (SiPM) as a signal source for optimum front-end design", *Nucl. Instr. Meth. Phys Res. Sec. A*, Volume 572, no. 1, pp. 416-418, 2007.